

# Nonperturbative quark-gluon thermodynamics at finite density\*

M.A. Andreichikov<sup>a,†</sup> M.S. Lukashov<sup>a,b,‡</sup> and Yu.A. Simonov<sup>a,§</sup>

<sup>a</sup> *Alikhanov Institute for Theoretical and Experimental Physics,  
B. Cheremushkinskya 25, 117218 Moscow, Russia*

<sup>b</sup> *Moscow Institute of Physics and Technology,  
Institutskiy per. 9, 141700 Dolgoprudny, Moscow Region, Russia*

December 3, 2021

## Abstract

Thermodynamics of the quark-gluon plasma at finite density is studied in the framework of the Field Correlator Method, where thermodynamical effects of Polyakov loops and colormagnetic confinement are taken into account. Having found good agreement with numerical lattice data for zero density, we calculate pressure  $P(T, \mu)$  for  $0 < \mu < 400$  MeV and  $150 < T < 1000$  MeV. For the first time the explicit integral form is found in this region, demonstrating analytic structure in the complex  $\mu$  plane. The resulting multiple complex branch points are found at the Roberge-Weiss values of  $\text{Im } \mu$ , with  $\text{Re } \mu$  defined by the values of Polyakov lines and colormagnetic confinement.

---

\*draft for **arXiv: v2** — December 3, 2021

<sup>†</sup>andreichicov@mail.ru

<sup>‡</sup>lukashov@phystech.edu

<sup>§</sup>simonov@itep.ru

# 1 Introduction

The new phenomenon of the quark-gluon plasma (QGP) was predicted in [1–3], and its properties were measured soon on the lattice [4–6]. Nowadays the QGP as an important stage in the heavy-ion collisions is widely recognized, see e.g. [7–11].

The recent accurate lattice measurements both in SU(3) [12–14] and in realistic  $2 + 1$  QCD theory [15, 16] have revealed the nontrivial character of thermodynamics for  $T < 600$  MeV, which includes strong nonperturbative ( $np$ ) interaction during the temperature transition region and beyond it.

At larger  $T$ ,  $T > 600$  MeV, one can hope to rely on the thermal perturbation theory (HTL) [17–19], however the infrared Linde problem implies an important role of  $np$  interaction also here [20, 21].

Therefore the  $np$  thermodynamics seems to be unavoidable in the whole  $T$  region.

The corresponding  $np$  approach, based on the vacuum fields, the Field Correlator Method (FCM), was originally formulated in [22–28], where the deconfining phase transition was associated with the vanishing of the confining correlator  $D^E$ , and later in [29, 30] it was shown, that another  $np$  correlator,  $D_1^E$ , is responsible for the dynamics of Polyakov loops. Moreover, the final form of the  $np$  thermodynamics in FCM was formulated in [29, 30] and compared with existing lattice data. At that time in the region beyond  $T_c$  only Polyakov lines have been taken into account, however a reasonable agreement within (20-25)% with the lattice data was achieved.

Recently another important ingredient of the  $np$  interaction in the region  $T > T_c$  was taken into account in addition to Polyakov lines – the Color Magnetic (CM) confinement is given by the spatial projection of the Wilson loop, and the  $np$  theory based on FCM for zero density (chemical potential) was finally formulated. In [31, 32] this theory was fully investigated in the case of SU(3) and compared to the accurate lattice data [12], showing a good agreement for  $p(T)$ ,  $I(T)$  both below and above  $T_c$ , and also in the character of transition. It is important, that a new effect was used in the subcritical region – the gradual vanishing of the confinement (the string tension  $\sigma$ ) when  $T$  approaches  $T_c$  from below.

This fact was found earlier on the lattice [33–36], and the use of this makes it unnecessary to exploit the Hagedorn string spectra.

In the quark-gluon case of  $2 + 1$  QCD the same type of the  $np$  approach (the account of Polyakov lines and CM confinement) was done for zero density and in the deconfined region in [37]. The resulting thermodynamic potentials in [37] are in a good agreement with the accurate lattice data [15, 16] in the region  $150 \text{ MeV} < T < 1000 \text{ MeV}$ , which implies, that the main part of dynamics is correctly taken into account. The confining region  $T \lesssim 150 \text{ MeV}$  was not treated in [37] and is in progress.

Meanwhile the region of nonzero density (chemical potential  $\mu$ ) is of the outmost importance. Indeed, the existing and planned experiments badly need the corresponding theoretical calculations of the QGP properties at nonzero  $\mu$ , whereas the lattice data are not directly available in this region. One particular example of an indirect information, provided by lattice data, is quark numbers susceptibilities  $\chi_n^X$ , which exist for long time [38], see [39, 40] for recent data. These data are important for comparison with experimental results in the freeze-out region [7–11]. It is a basic feature of our approach, that the nonzero density is easily incorporated into the formalism, and the analysis of the complex chemical potential can be done in the whole plane of complex  $\mu$ . In this way one can find all singularities in this plane and find their dynamical origin. This can be closely connected to the possible existence of critical and quasicritical points in  $(\mu, T)$  plane, and is therefore of utmost importance.

Our  $np$  approach to the case of the finite density was formulated in [41, 42], see also [43] for a review, where in the QGP only the Polyakov line interaction was taken into account, and

the whole temperature transition curve in the  $\mu - T$  plane was found.

In addition the curvature of  $T_c(\mu)$  was found in [41, 42],  $\kappa_2 = 0.0110(3)$ , which is in a good agreement with existing lattice and freeze-out data, see Fig. 1 in [44].

However, the CM confinement was not taken into account in [41, 42], and the experience of our latest calculations in  $SU(3)$  and QCD shows, that it is important and can seriously improve the accuracy of the results.

The purpose of the present paper is to incorporate in our calculations of  $np$  thermodynamics for finite density the effects CM confinement and to produce the function of pressure  $p(T, \mu)$ , in the temperature interval  $0.2 < T < 1.0$  GeV. It is also interesting to investigate the properties of  $p(T, \mu)$  in the whole complex plane of  $\mu$  and to compare with known lattice information.

The paper is organized as follows. In the next section the main equations of our method are presented. In section 3 the properties of the thermodynamical potentials are discussed, and in section 4 the case of an arbitrary CM interaction is treated, while the section 5 contains numerical results and the section 6 is devoted to the discussion and an outlook.

## 2 Thermodynamic potentials of quark-gluon plasma at finite density

We are using below the same gauge and relativistic invariant formalism, based on the path integral formalism, which was formulated in [22–30], and exploited in the  $SU(3)$  case in [37]. The basic interaction of a quark or a gluon can be expressed via world lines affected by the vacuum fields and finally written in the form of Wilson–lines and loops. One can consider [24, 29] as a detailed review of FCM technique applied to the  $np$  quark-gluon thermodynamics at finite temperature and density. It is essential that in the deconfined phase two basic interactions define the quark and gluon dynamics: the colorelectric (CE) one, contained in the Polyakov line  $L(T)$ , and the colormagnetic (CM) interaction in the spatial projection on the Wilson loop. The CE part is expressed via the  $np$  part of the CE field correlator  $D_1^E(\tau)$ , while perturbative part of  $D_1$  yields color Coulomb potential. The CM part is defined by the CM field correlator  $D^H(z)$ , yielding the spatial string tension  $\sigma_s(T) = \frac{1}{2} \int D^H(z) d^2 z$ . As it was shown within FCM [21]  $\sigma_s(T) = O(T^2)$  and is important in the whole region  $T \geq T_c$ .

Using the  $T$  dependent path integral (world line) formalism one can express thermodynamic potentials via the Wilson loop integral, e.g. for the gluon pressure one has [21, 32]

$$P_{gl} = 2(N_c^2 - 1) \int_0^\infty \frac{ds}{s} \sum_{n=1,2,\dots} G^{(n)}(s), \quad (1)$$

where we use Feynman-Fock-Schwinger (FSF) formalism with Schwinger proper time  $s$ , and  $G^{(n)}(s)$  are the winding (Matsubara) path integrals

$$G^{(n)}(s) = \int (Dz)_{on}^w e^{-K} \langle \text{tr}_a W(C_n) \rangle, \quad (2)$$

where  $K = \frac{1}{4} \int_0^s \left( \frac{dz_\mu(\tau)}{d\tau} \right)^2 d\tau$  according to the FSF method and  $W(C_n)$  is the Wilson loop defined for the gluon path  $C_n$ , which has both temporal (i4) and spacial projections (ij). It is important, that the CE and CM field strengths in  $T > T_c$  region correlate very weakly during the gauge-invariant field correlator in adjoint representation  $\langle E_i(x) B_k(y) \Phi(x, y) \rangle \approx 0$  (see [29, 30] for a discussion of this point) and therefore both CE and CM projections of the  $\text{tr}_a W(C_n)$  can be factorized as shown in [32]

$$\langle \text{tr}_a W(C_n) \rangle = L_{\text{adj}}^{(n)}(T) \langle W_3 \rangle. \quad (3)$$

Inserting (3) in (2), one can integrate out the  $z_4$  part of the path integral  $(Dz)_{on}^w = (Dz_4)_{on}^w D^3 z$ , and write the result as

$$G^{(n)}(s) = G_4^{(n)}(s) G_3(s); \quad G_4^{(n)}(s) = \int (Dz)_{on}^w e^{-K} L_{adj}^{(n)} = \frac{1}{2\sqrt{4\pi s}} e^{-n^2/4T^2 s} L_{adj}^{(n)}. \quad (4)$$

This basic factorization holds also for quarks and will be used below for both quarks and gluons.

#### A) GLUONS

Following the previous discussion we start with the gluon pressure and write it in the same form, as was written in [29,30,32,43], where gluon is moving in the vacuum field, which creates both Polyakov loops (via interaction  $V_1(\infty, T)$ ) and confinement for the spatial loops

$$P_{gl} = \frac{N_c^2 - 1}{\sqrt{4\pi}} \int_0^\infty \frac{ds}{s^{3/2}} G_3(s) \sum_{n=0,1,2,\dots} e^{-\frac{n^2}{4T^2 s}} L_{adj}^{(n)}. \quad (5)$$

Here  $G_3(s)$  is the gluon Green's function in the 3d spatial projection. It can be written in the free case as  $G_3^{(0)}(s) = \frac{1}{(4\pi s)^{3/2}}$ , and when the interaction in the loop has the form of an oscillator, it can be written as [32]

$$G_3^{osc}(s) = \frac{1}{(4\pi s)^{3/2}} \frac{(M_0^2 s)}{\sinh(M_0^2 s)}, \quad (6)$$

where  $M_0$  is connected to the oscillator parameters. In [32] the following approximate form was suggested in the realistic case of the linear confinement

$$G_3^{lin}(s) = \frac{1}{(4\pi s)^{3/2}} \sqrt{\frac{(M_{adj}^2 s)}{\sinh(M_{adj}^2 s)}}. \quad (7)$$

The form (7) with  $M_{adj} \cong 2M_D$  ( $M_D$  is the gluon Debye mass) used in [32] provides the pressure  $p(T)$  and trace anomaly  $I(T)$  in good agreement with lattice data [12]. As shown in [29,30,43],  $L_{adj}^{(n)} \cong (L_{adj}(T))^n$  for  $T \lesssim 1$  GeV, and  $L_{adj}(T) = \exp\left(-\frac{9V_1(\infty, T)}{8T}\right)$ . As shown in [32], the resulting  $L_{adj}(T)$ , which is close to the lattice measurement values, yields realistic thermodynamic potentials.

#### B) QUARKS

For quarks one can write, following [29,30,41,42] the same form as in (5), but augmented by the quark mass term  $e^{-m_f^2 s}$  and the density term  $\cosh \frac{\mu n}{T}$ .

$$P_q = \sum_{m_q} P_q^{(f)}, \quad P_q^{(f)} = \frac{4N_c}{\sqrt{4\pi}} \int_0^\infty \frac{ds}{s^{3/2}} e^{-m_f^2 s} S_3(s) \sum_{n=1,2,\dots} (-)^{n+1} e^{-\frac{n^2}{4T^2 s}} \cosh\left(\frac{\mu n}{T}\right) L_f^{(n)}. \quad (8)$$

Here  $S_3(s)$  is, similarly to  $G_3(s)$ , the 3d quark Green's function, which can be approximated in the same way as in (7),

$$S_3^{lin}(s) = \frac{1}{(4\pi s)^{3/2}} \sqrt{\frac{(M_f^2 s)}{\sinh(M_f^2 s)}}, \quad (9)$$

with the relation  $M_{adj}^2 = \frac{9}{4} M_f^2$ .

Eqs.(5), (8) with definitions (7), (9) are our basis for the analysis and calculations to be done in the following sections.

### 3 Properties of thermodynamic potential at finite density

In what follows we shall be interested in the full pressure  $P(T, \mu) = P_{gl}(T) + P_q(T, \mu)$ , where  $P_q(T, \mu)$  is given in (8, 9). In addition on the lattice one also considers quark number susceptibilities  $\chi_{m,n}(T)$ , according to the standard definitions

$$\Delta P(T, \mu) = P(T, \mu) - P(T, \mu = 0) \quad (10)$$

$$\frac{\Delta P(T, \mu)}{T^4} = \sum_{i+j+k=\text{even}} \frac{\chi_{ijk}(T)}{i!j!k!} \hat{\mu}_u^{(i)} \hat{\mu}_d^{(j)} \hat{\mu}_s^{(k)}, \quad (11)$$

where  $\hat{\mu} = \frac{\mu}{T}$ .

In addition it is useful to obtain the baryon density  $n(T, \mu_B)$

$$n(T, \mu_B) = \frac{\partial \Delta P(T, \mu_B)}{\partial \mu_B}, \mu_B \cong 3\mu. \quad (12)$$

The analysis of  $\chi_{mn}$  in lattice data allows to obtain information on the possible critical point  $T_c(\mu)$ .

In our case, since our  $P(T, \mu)$  has a definite analytic form, one can search for  $T_c(\mu)$  explicitly. Indeed, after the integration over  $ds$ , our  $P(T, \mu)$  is a sum over  $n$ , which diverge at some value of  $\mu = \mu_{cr}(T) \simeq 0.51 \text{ GeV}$ .

It is convenient to represent  $P_q^{(f)}$  in (8) in the form

$$\frac{1}{T^4} P_q^{(f)} = \frac{N_c}{4\pi^2} \sum_{n=1}^{\infty} \frac{(-1)^{n+1}}{n^4} e^{-\frac{nV_1(\infty, T)}{2T}} \cosh \frac{\mu n}{T} \cdot \Phi_n(T), \quad (13)$$

where  $\Phi_n(T)$  is

$$\frac{\Phi_n(T)}{n^4} = \frac{(4\pi)^{3/2}}{T^4} \int_0^{\infty} \frac{ds}{s^{3/2}} e^{-m_f^2 s} S_3(s) e^{-\frac{n^2}{4T^2 s}}. \quad (14)$$

One can use for  $S_3(s)$  different forms. E.g., if one expands  $S_3(s)$  in terms, corresponding to the series over bound states with masses  $m_\nu$  and wave functions  $\psi_\nu(x)$ , then one can write  $S_3(s)$  as in Eq. (34) of [32], namely

$$S_3(s) = \frac{1}{\sqrt{\pi s}} \sum_{\nu=0,1,\dots} \psi_\nu^2(0) e^{-m_\nu^2 s}. \quad (15)$$

In the case, when one represents the colormagnetic confinement by the oscillator potential, one has

$$S_3^{osc}(s) = \frac{1}{(4\pi s)^{3/2}} \frac{(M_0^2 s)}{\sinh(M_0^2 s)}. \quad (16)$$

Finally, when one approximates the linear CM confinement as in (9), then one can write the following form, which approximates  $S_3^{osc}$  and  $S_3^{lin}$  with the accuracy of (5-10)% in the region  $M_0^2 s$

$$S_3^{lin}(s) \cong \frac{1}{(4\pi s)^{3/2}} \sqrt{\frac{(M^2 s)}{\sinh(M^2 s)}} \approx \frac{1}{(4\pi s)^{3/2}} e^{-\frac{M^2 s}{4}}. \quad (17)$$

In this case  $\Phi_n(T)$  can be calculated explicitly, namely.

$$\Phi_n(T) = \frac{8n^2 \bar{M}^2}{T^2} K_2 \left( \frac{\sqrt{\bar{M}^2 n}}{T} \right), \quad \bar{M} = \sqrt{m_f^2 + \frac{M^2}{4}}. \quad (18)$$

Let us introduce the following functions

$$\xi_1 = \sum_n \frac{(-)^{n+1}}{n^2} L^n e^{\pm \frac{\mu n}{T}} K_2 \left( \frac{\bar{M} n}{T} \right), \quad (19)$$

One can use the integral representation

$$K_\nu(z) = \frac{\left(\frac{z}{2}\right)^\nu \Gamma\left(\frac{1}{2}\right)}{\Gamma\left(\nu + \frac{1}{2}\right)} \int_0^\infty e^{-z \cosh t} \sinh^{z\nu} t \, dt, \quad (20)$$

which allows to sum up all terms in the sum over  $n$ , namely

$$\xi_1^\pm = \frac{4}{3} \left( \frac{\bar{M}}{2T} \right)^2 \int_0^\infty \frac{u^4 du}{\sqrt{1+u^2}} \frac{1}{1 + \exp\left(\frac{\bar{M}}{T} \sqrt{1+u^2} + \frac{V_1}{2T} \mp \frac{\mu}{T}\right)}, \quad (21)$$

and the pressure can be written as

$$\frac{1}{T^4} P_q^{(f)} = \frac{2N_c}{\pi^2} \left[ \frac{1}{2} (\xi_1^+ + \xi_1^-) \right] \quad (22)$$

One can see, that (21) has no singularities at  $\mu$  real, but  $\xi_i$  may get a singularity for  $\text{Im} \frac{\mu}{T} = \pi$  due to vanishing of the denominator in (21) at  $u = 0$ . We can add to  $\frac{V_1(\infty, T)}{2T}$  the complex phase of the Polyakov loop  $i\phi$ , where  $\phi$  can assume  $Z(3)$  values  $\phi_k = \frac{2\pi}{3}k$ ,  $k = 0, \pm 1$  and the factor in the exponent in (21) at  $u = 0$  has the form

$$a_\pm = \exp \left( \pm \frac{\mu_R + i\mu_I}{T} + i \frac{2\pi}{3} k + \frac{V_1(\infty, T)}{2T} + \frac{\bar{M}(T)}{T} \right). \quad (23)$$

Note, that for the prefactor of the exponent in (21) be equal to  $(-1)$  the imaginary part of  $\mu$  should be equal

$$\frac{\mu_I}{T} = \frac{\pi}{3}(2n+1), \quad n = 0, \pm 1, \pm 2, \dots \quad (24)$$

These are exactly the Roberge-Weiss values [45].

This situation may explain the appearance of the Roberge-Weiss singularities [45], see [46], [47] for a physical and numerical analysis.

As a result, in the normal situation with  $\mu$  and  $L_f$  real the singularity is absent, implying the absence of the critical point  $T_c(\mu)$ . This result is in line with the lattice analysis in [39, 40, 48], where no sign of  $T_c$  was observed in quark numbers susceptibilities. Note, however, that our conclusion refers to the purely  $np$  contribution, where the perturbative gluon and quark exchanges are absent. Moreover, we have not taken into account a possible density modification of the vacuum averages, in particular of the confinement parameters.

## 4 The case of arbitrary CM interaction

In the general case of the CM interaction, which produces in 3d the spectrum with eigenvalues  $m_\nu^2$  and eigenfunctions  $\psi_\nu(\rho)$ , one can write as in (15)

$$S_3(s) = \frac{1}{\sqrt{\pi s}} \sum_{\nu=0,1,\dots} \psi_\nu^2(0) e^{-m_\nu^2 s} \quad (25)$$

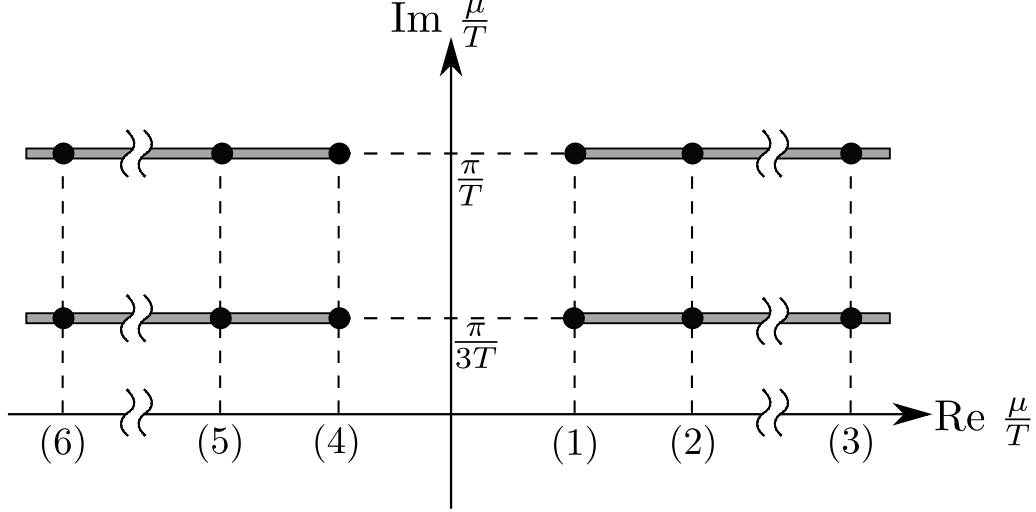


Figure 1: Roberge-Weiss singular points and cuts in the complex plane of  $\mu$ . Points 1,2,3,4,5, and 6 are, respectively,  $\left(\frac{V_1}{2T} + \frac{M_0}{T}\right)$ ,  $\left(\frac{V_1}{2T} + \frac{M_0\sqrt{3}}{T}\right)$ ,  $\left(\frac{V_1}{2T} + \frac{M_\nu}{T}\right)$ ,  $-\left(\frac{V_1}{2T} + \frac{M_0}{T}\right)$ ,  $-\left(\frac{V_1}{2T} + \frac{M_0\sqrt{3}}{T}\right)$ , and  $-\left(\frac{V_1}{2T} + \frac{M_\nu}{T}\right)$ . In the lower half plane the points are mirror-reflected of the axis  $\text{Re}(\mu/T)$ .

For  $\Phi_n(T)$  in (13) one obtains

$$\frac{\Phi_n(T)}{n^4} = \frac{8\pi}{T^4} \sum_{\nu} \psi_{\nu}^2(0) \int_0^{\infty} \frac{ds}{s^2} e^{-\bar{M}_{\nu}^2 s - \frac{n^2}{4T^2 s}} = \frac{32\pi}{T^3} \sum_{\nu} \psi_{\nu}^2(0) \bar{M}_{\nu} \frac{K_1\left(\frac{n\bar{M}_{\nu}}{T}\right)}{n}, \quad (26)$$

where  $\bar{M}_{\nu}^2 = m_f^2 + m_{\nu}^2$ . The  $P_q^{(f)}$  acquire the form

$$\frac{P_q^{(f)}}{T^4} = \frac{8N_c}{\pi T^3} \sum_n \psi_{\nu}^2(0) \bar{M}_{\nu} \sum_n \frac{(-)^{n+1}}{n} K_1\left(\frac{n\bar{M}_{\nu}}{T}\right) L^n \cosh \frac{\mu n}{T}. \quad (27)$$

Now using the representation

$$K_1\left(\frac{n\bar{M}_{\nu}}{T}\right) = \frac{n\bar{M}_{\nu}}{T} \int_0^{\infty} e^{-\frac{n\bar{M}_{\nu}}{T} \cosh t} \sinh^2 t \, dt, \quad (28)$$

one can sum up the geometrical progression in  $n$  with the result

$$\frac{P_q^{(f)}}{T^4} = \frac{8N_c}{\pi T^4} \sum_{\nu=0}^{\infty} \psi_{\nu}^2(0) \bar{M}_{\nu}^2 \int_0^{\infty} \sinh^2 t \, dt \frac{1}{2} \left( \frac{c_+}{1+c_+} + \frac{c_-}{1+c_-} \right), \quad (29)$$

where  $c_{\pm} = \exp \left\{ -\frac{\bar{M}_{\nu}}{T} \cosh t - \frac{V_1}{2T} \pm \frac{\mu}{T} \right\}$ .

It is interesting to find the exact position and the character of singularities in the complex  $\mu$  plane, shown in Fig. 1. To this end we are writing  $\frac{\mu}{T}$  in the neighborhood of the point in Fig. 1 with imaginary and real parts  $i\pi$  and  $\frac{\mu_R}{T}$  respectively as

$$\frac{\mu}{T} = i\pi + \frac{M_{\nu} + V_1/2}{T} + \frac{M_{\nu}}{T} y. \quad (30)$$

The integral (29) as a function of  $y$  is proportional to the function  $f(y)$ ,

$$f(y) = \int_0^{\infty} \frac{t^2 dt F(t)}{t^2 - 2y + O(t^2 y, t^4 y^2)}, \quad (31)$$

where we have separated the region of small  $t$ , contributing to the singularity, and  $F(t \rightarrow 0) = \text{const.}$

One can easily see in (31), that  $f(y)$  has a square root singularity near  $y = 0$  and the cut  $\text{Re } y \geq 0$ , with the discontinuity

$$f(y + i\delta) - f(y - i\delta) = i\sqrt{2y}F(\sqrt{2y}). \quad (32)$$

Note, that the branch points  $y = 0$  occur for every  $M_\nu, \nu = 0, 1, 2, \dots$  and this situation is similar to the two-body thresholds in the energy plane with ever increasing number of particles.

In the case of the oscillator-type CM interaction one has

$$\psi_\nu^2(0) = \frac{M_0^2}{4\pi}, \quad \bar{M}_\nu^2 = m_f^2 + M_0^2(2\nu + 1), \quad M_0 \approx 2\sqrt{\sigma_s}. \quad (33)$$

One can see in (29) that for not large  $T$  the lowest in  $\nu$  terms dominate.

In the free limit one has  $\sum_\nu \psi_\nu^2(0) \rightarrow \int \frac{d^2 p}{(2\pi)^2}$ ,  $\bar{M}_\nu^2 = 2p^2 + m_f^2$ , and for  $\Phi_n^{(\text{free})}$  one obtains from (26)

$$\frac{\Phi_n^{(\text{free})}(T)}{n^4} = \frac{8}{n^4} \int_0^\infty z^2 K_1(z) dz = \frac{16}{n^4}. \quad (34)$$

As a result the limit of no CM interaction is

$$\frac{P_q^{(f)}(\text{no CM})}{T^4} = \frac{4N_c}{\pi^2} \sum_{n=1}^\infty \frac{(-)^{n+1}}{n^4} L^n \cosh \frac{\mu n}{T}, \quad (35)$$

which reduces to the expression, found in [41, 42]

$$\frac{P_q^{(f)}(\text{no CM})}{T^4} = \frac{1}{\pi^2} \left[ \Psi \left( \frac{\mu - \frac{V_1}{2}}{T} \right) + \Psi \left( -\frac{\mu + \frac{V_1}{2}}{T} \right) \right], \quad (36)$$

where

$$\Psi(a) = \int_0^\infty \frac{z^4 dz}{\sqrt{z^2 + \nu^2}} \frac{1}{\exp(\sqrt{z^2 + \nu^2} - a) + 1}, \quad (37)$$

and  $\nu = \frac{m_q}{T}$ .

## 5 Numerical calculations and comparison to lattice data

In this section we present results of calculations for the total pressure

$$P(\mu, T) = P_{gl}(T) + \sum_{m_q(i)} P_q^{(f)}(\mu_i, T), \quad (38)$$

where  $P(\mu_f, T)$  in general depends on the  $\mu_f$  for a given flavor. Below we consider the simplest case of equal  $\mu_f = \mu$ , where  $f = u, d, s$ , and the quark masses  $m_u = m_d = 0$ ,  $m_s = 0.1 \text{ GeV}$ .  $P_{gl}(T)$  is given by Eq.(5) and is  $\mu$ -independent in our approximation of no interaction between quarks and gluons. As for  $P_q(T, \mu)$  we shall use two different strategies for its numerical calculation.

In the first case one exploits the general form of Eq. (13) and approximates the linear confinement case of  $S_3^{lin}(s)$  as in Eq. (17) with  $\bar{M} = \sqrt{m_f^2 + \frac{M_0^2}{4}}$ , and  $M_0 = b\sqrt{\sigma_s}$ , where  $b$  is of the order of 1. As a result one obtains  $P_q$  as in Eq. (21) with  $\xi_1$  given in Eq. (20). The resulting values of  $\frac{P(0, T)}{T^4}$  for  $\mu = 0$  are given in Fig. 2 for  $b = 0, 2.0, 3.0, 3.5$  in comparison



with lattice data from [16]. Note, that for the Polyakov loop  $L_f(T) = \exp(-V_1(T)/2T)$  we are using as in Eq. (5) and Eq. (13) the same values as in [37, 41–43], with  $L_{adj} = (L_f)^{9/4}$ , namely

$$V_1(T) = \frac{0.175 \text{ GeV}}{1.35 \frac{T}{T_0} - 1}, \quad T_0 = 0.16 \text{ GeV} \quad (39)$$

in the interval  $0.16 \text{ GeV} < T < 1 \text{ GeV}$ .

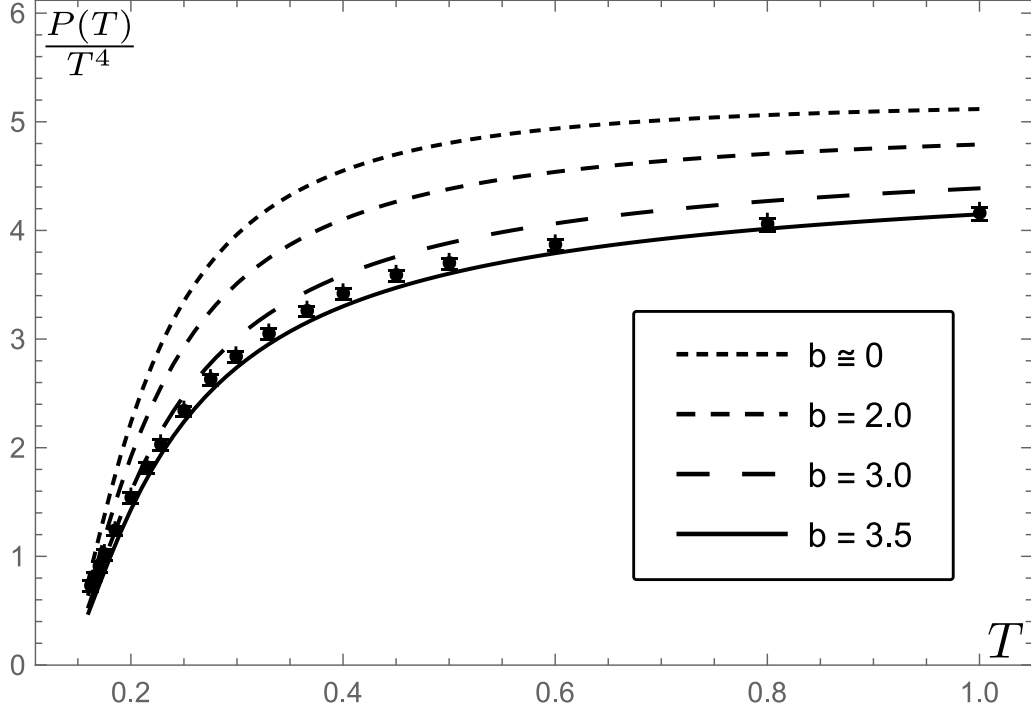


Figure 2: The pressure  $\frac{P(T)}{T^4}$  with  $M_0 = b\sqrt{\sigma_s}$  ( $\mu = 0$ ), where  $b = 0, 2.0, 3.0, 3.5$  (from top to bottom), – filled dots are for the lattice data from [16].

The resulting values of  $L_f(T)$  are in the same domain as the lattice data of [50–53] for  $T < 0.5 \text{ GeV}$ , while at higher  $T$  our  $L_f$  is smaller due to necessary renormalization, because of different definitions, see [54] for the discussion of this point. Of special importance is the possible  $\mu$ -dependence of  $L_f(T)$ , which can occur due to density dependence of vacuum fields, as well as due to quark-quark interaction. In our approach at this stage we disregard this dependence, which is partly supported by lattice data [55]. As a result one can see in Fig. 2 a reasonable agreement of our curve for  $P(T, \mu = 0)$  for  $M_0 = 3.5\sqrt{\sigma_s}$  with lattice data from [16], and we shall exploit this value for  $\mu > 0$ . In Fig. 3 we show the behavior of  $P(T, \mu)$  for  $\mu = 0, 0.2, 0.4 \text{ GeV}$ . One can see a maximum appearing at large  $\mu$  around  $T = 0.25 \text{ GeV}$ .

At the same time we are using another strategy, exploiting Eq. (27) for  $P_f(T, \mu)$  with the values  $\psi_\nu$  and  $M_\nu$  from (33), corresponding to the oscillator CM interaction. The resulting behavior of the  $P(T, \mu)/T^4$  is shown in Fig. 4 for  $\mu = 0, 0.2, 0.4 \text{ GeV}$ , where also the case of  $\mu = 0$  can be compared to lattice data [16]. One can see a reasonable agreement with lattice data for  $\mu = 0$  and an agreement with the results of Fig. 3, obtained in the first approach, which can be considered as additional support of our results.

## 6 Conclusions and prospectives.

We have considered above in the paper the properties of the quark-gluon medium in the temperature interval  $0.15 \text{ GeV} < T < 1 \text{ GeV}$  and for the chemical potential  $\mu = 0, 0.2$  and  $0.4 \text{ GeV}$ .

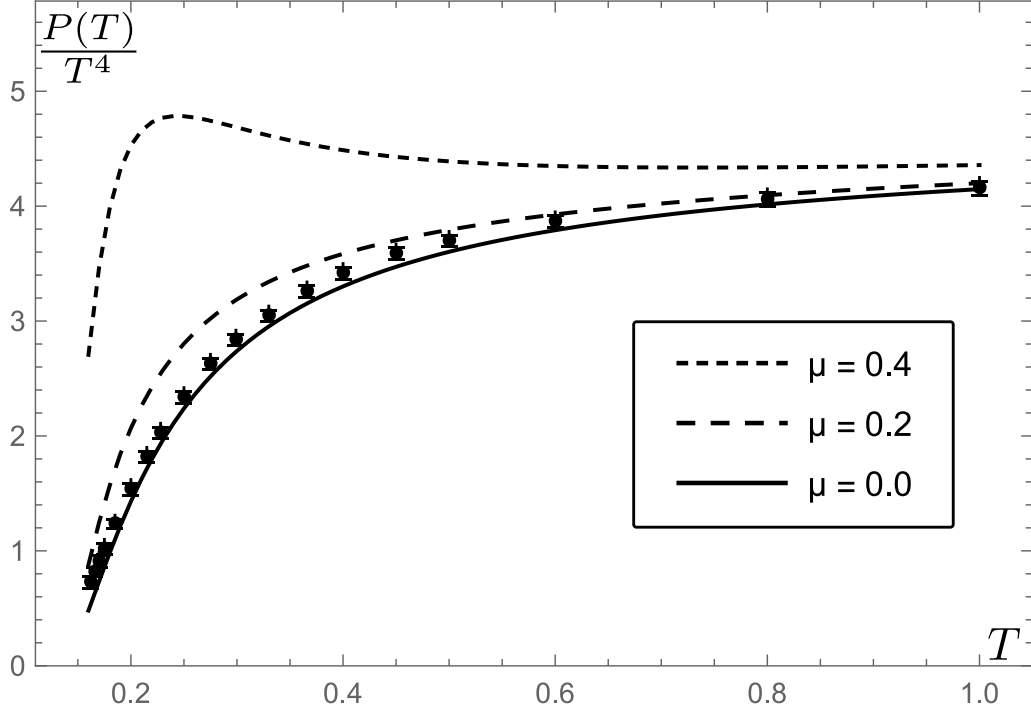


Figure 3: The pressure  $\frac{P(T)}{T^4}$  with  $M_0 = 3.5 \sqrt{\sigma_s}$  for  $\mu = 0.0, 0.2, 0.4$  (from bottom to top), – filled dots are for the lattice data from [16].

We have taken into account only the  $np$  part of interaction, which is connected with the vacuum fields and we have disregarded in this first part of study the effects of the continuous phase transition(crossover), which mostly proceed in the lower temperature interval, and will be considered elsewhere. The main reason for our choice of dynamics is the fact, that the CM confinement and Polyakov interaction ( $V_1(T)$ ) are most strong in this region and moreover CM confinement is growing with temperature.

As it is, we have analyzed the behavior of  $P(T, \mu)$  and up to  $\mu = 0.4 \text{ GeV}$  and have not found any discontinuous effects in this area. It is seen in Figs. 2-4 that the pressure has a smooth behavior, while the peak in  $P(T, \mu)$  appears at smaller  $T$  with increasing  $\mu$ . It is important, that the series over  $n$  in Eq. (13) is convergent for these values of  $\mu$ , as it was checked both via the sum over eigenstates, Eq. (27), and via the linear approximation, Eq. (17). At the same time we have studied above the analytic properties of thermodynamic potentials in the complex  $\mu$  plane and have found sequences of branch points with cuts, going outwards, see Fig. 1. These singularities and cuts are dynamically explained by the Polyakov line interaction  $V_1(T)$  and CM confinement eigenvalues  $M_\nu$ , as it is shown in Eq. (23), indeed at the branch point one has  $\pm\mu = M_\nu + \frac{V_1(T)}{2}$ . We have not studied above the explicit consequences of these singularities for the convergence of the series and the possibility of quasicritical points, leaving this topic for the future.

---

The authors are grateful to V.G. Bornyakov for useful discussions. This work was done in the framework of the scientific project, supported by the Russian Scientific Fund, grant #16-12-10414.

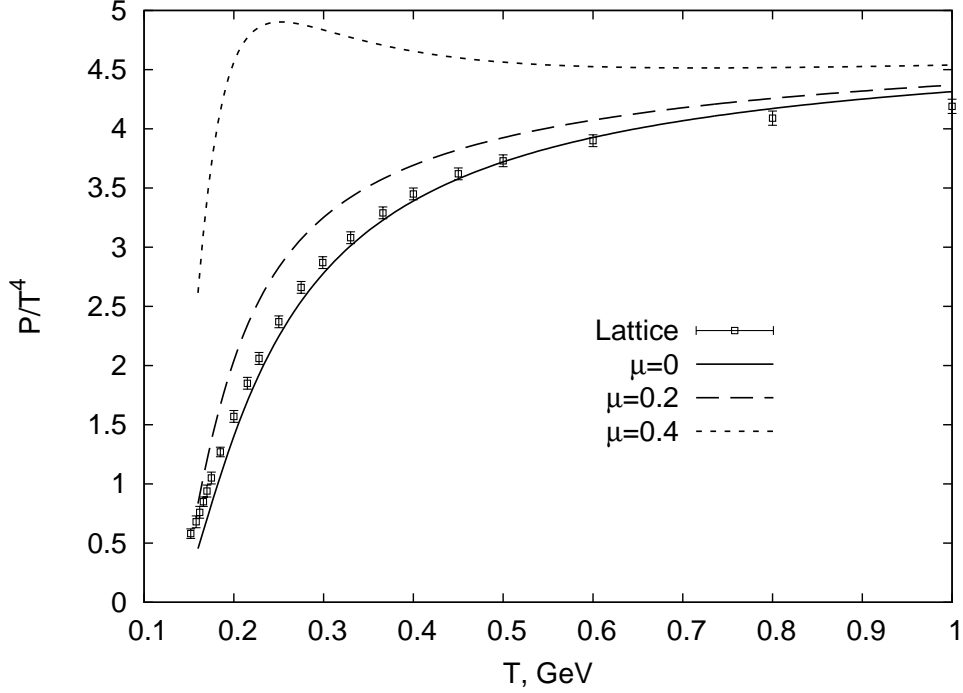


Figure 4: The pressure  $\frac{P(T)}{T^4}$  with  $M_0 = 3.5 \sqrt{\sigma_s}$  for  $\mu = 0.0, 0.2, 0.4$  (from bottom to top), empty squares with error bars are for the lattice data from [16].

## References

- [1] J. C. Collins, M. J. Perry, Phys. Rev. Lett. **34**, 1353 (1975).
- [2] N. Cabibbo, G. Parisi, Phys. Lett. **B 59**, 67 (1975).
- [3] E. V. Shuryak, Sov. Phys. JETP **47**, 212 (1978).
- [4] M. Creutz, Phys. Rev. **D 21**, 2308 (1980).
- [5] L. D. McLerran, B. Svetitsky, Phys. Lett. **B 98**, 195 (1981).
- [6] J. Kuti, J. Polonyi, K. Szlachanyi, Phys. Lett. **B 98**, 199 (1981).
- [7] P. Braun-Munzinger, V. Koch, Th. Schäfer and J. Stachel, Phys. Rept. **621**, 76 (2016) [arXiv:1510.00442 [nucl-th]].
- [8] A. Andronic, P. Braun-Munzinger, K. Redlich and J. Stachel, J. Phys.: Conf. Ser. **779**, 012012 (2017) [arXiv:1611.01347 [nucl-th]].
- [9] M. Albright, J. Kapusta and C. Young, Phys. Rev. **C 90**, 024915 (2014) [arXiv:1404.7540 [nucl-th]].
- [10] M. Albright, J. Kapusta and C. Young, Phys. Rev. **C 92**, 044904 (2015) [arXiv:1506.03408 [nucl-th]].
- [11] J. Cleymans, H. Oeschler, K. Redlich and S. Wheaton, Phys. Rev. **C 73**, 034905 (2006) [arXiv:hep-ph/0511094].
- [12] Sz. Borsanyi, G. Endrödi, Z. Fodor, A.D. Katz and K.K. Szabo, JHEP, **2012**(07): 056 (2012), [arXiv:1204.6184 [hep-lat]].

- [13] L. Giusti and M. Pepe, Phys. Lett. **B 769**, 385 (2017) [arXiv:1612.00265 [hep-lat]].
- [14] L. Giusti and M. Pepe, PoS (LATTICE-2016): 061 [arXiv:1612.02337 [hep-lat]].
- [15] A. Bazavov, T. Bhattacharya, G. De Tar, et al, (Hot QCD Collaboration), Phys. Rev. **D 90**, 094503 (2014) [arXiv:1407.6387 [hep-lat]].
- [16] Sz. Borsanyi, G. Endrödi, Z. Fodor, et al., JHEP **2010**(11): 077 (2010) [arXiv:1007.2580 [hep-lat]].
- [17] E. Braaten and R.D. Pisarski, Phys. Rev. Lett. **64**, 1338 (1990).
- [18] J.O. Andersen, E. Braaten and M. Strickland, Phys. Rev. Lett. **83**, 2139 (1999) [arXiv:hep-ph/9902327].
- [19] N. Haque, A. Bandyopadhyay, J.O. Andersen, M.G. Mustafa, M. Strickland, et al., JHEP **2014**(05): 027 (2014) [arXiv:1402.6907 [hep-ph]].
- [20] A.D. Linde, Phys. Lett. **B 96**, 289 (1980).
- [21] Yu.A. Simonov, arXiv:1605.07060 [hep-ph].
- [22] Yu.A. Simonov, JETP Lett. **54**, 249 (1991).
- [23] Yu.A. Simonov, JETP Lett. **55**, 627 (1992).
- [24] Yu.A. Simonov, Phys. At. Nucl. **58**, 309 (1995) [hep-ph/9311216].
- [25] N.O. Agasian, JETP Lett. **57**, 208 (1993).
- [26] N.O. Agasian, JETP Lett. **71**, 43 (2000).
- [27] H.G. Dosch, H.J. Pirner, Yu.A. Simonov, Phys. Lett. **B 349** 335 (1995).
- [28] Yu.A. Simonov, in: “*Varenna-1995: Selected Topics in Nonperturbative QCD*”, Eds. A.Di Giacomo and D. Diakonov (IOS Press, Italy, 1996), p. 319 [hep-ph/9509404].
- [29] Yu.A. Simonov, Ann. Phys. **323**, 783 (2008) [arXiv: hep-ph/0702266].
- [30] E.V. Komarov, Yu.A. Simonov, Ann. Phys. **323**, 1230 (2008) [arXiv:0707.0781 [hep-ph]].
- [31] N.O. Agasian, M.S. Lukashov and Yu.A. Simonov, Mod. Phys. Lett. **A 31**, 1050222 (2016) [arXiv:1610.01472 [hep-lat]].
- [32] N.O. Agasian, M.S. Lukashov and Yu.A. Simonov, Eur. Phys. J. **A 53**: 138 (2017) [arXiv:1701.07959 [hep-ph]].
- [33] O. Kaczmarek, F. Karsch, E. Laermann and M. Lutgemeier, Phys. Rev. **D 62** (2000) 034021 [arXiv:hep-lat/9908010].
- [34] P. Bicudo and N. Cardoso, Phys. Rev. **D 85**, 077501 (2012) [arXiv:1111.1317 [hep-lat]].
- [35] P.Bicudo and N.Cardoso, arXiv:1608.07742 [hep-lat].
- [36] P. Cea, L. Cosmai, F. Cuteri and A. Papa, JHEP **2016**(06): 033 (2016) [arXiv:1511.01783 [hep-lat]].

- [37] M.S. Lukashov and Yu.A. Simonov, JETP Letters **105**, 691 (2017) [arXiv: 1703.06666 [hep-ph]].
- [38] S.A. Gottlieb, W. Lin, D. Toussaint, R.L. Reken and R.L. Sugar, Phys. Rev. Lett. **59**, 2247 (1987).
- [39] M. D’Elia, G. Gagliardi and F. Sanfilippo, Phys. Rev. **D 95**, 094503 (2017) [arXiv:1611.08285 [hep-lat]].
- [40] A. Bazavov, H.-T. Ding, P. Hegde, et al., Phys. Rev. **D 95**, 054504 (2017) [arXiv:1701.04325 [hep-lat]].
- [41] Yu.A. Simonov, M.A. Trusov, JETP Lett. **85**, 598 (2007) [arXiv:hep-ph/0703228].
- [42] Yu.A. Simonov, M.A. Trusov, Phys. Lett. **B 650**, 36 (2007) [arXiv:hep-ph/0703277].
- [43] A.V. Nefediev, Yu.A. Simonov and M.A. Trusov, Int. J. Mod. Phys. **E 18**, 549 (2009) [arXiv:0902.0125 [hep-ph]].
- [44] C. Bonati, M. D’Elia, M. Mariti, M. Mesiti and F. Negro, Proceedings of CPOD-2016, C-16-05-30.7 (2016) [arXiv:1610.03338 [hep-lat]].
- [45] A. Roberge and N. Weiss, Nucl. Phys. **B 275**, 734 (1986).
- [46] C. Bonati, P. De Forcrand, M. D’Elia, O. Philipsen and F. Sanfilippo, Phys. Rev. **D 90**, 074030 [arXiv:1408.5086].
- [47] R. Falcone, E. Laermann and M.P. Lombardo, PoS (LATTICE-2010): 183 [arXiv:1012.4694 [hep-lat]].
- [48] C. De Tar, L. Levkova, S. Gottlieb, et al., Phys. Rev. **D 81**, 114504 (2010) [arXiv:1003.5682 [hep-lat]].
- [49] S. Gupta, N. Karthik and P. Majumdar, Phys. Rev. **D 90**, 034001 (2014) [arXiv:1405.2206 [hep-lat]].
- [50] A. Bazavov, N. Brambilla, H.-T. Ding, et al., Phys. Rev. **D 93**, 114502 (2016) [arXiv:1603.06637 [hep-lat]].
- [51] P. Petreczky, H.-P. Schadler, Phys. Rev. **D 92**, 094517 (2015) [arXiv:1509.07874 [hep-lat]].
- [52] O. Kaczmarek, F. Zantow, Phys. Rev. **D 71**, 114510 (2005) [arXiv:hep-lat/0503017].
- [53] S. Borsanyi, S. Durr, Z. Fodor, et al., JHEP **2012**(08): 126 (2012) [arXiv:1205.0440 [hep-lat]].
- [54] Yu.A. Simonov, Phys. Lett. **B 619**, 293 (2005) [hep-ph/0502078].
- [55] J. Takahashi, K. Nagata, T. Saito, et al., Phys. Rev. **D 88**, 114504 (2013) [arXiv:1308.2489 [hep-lat]].